#29

OBLON
SPIVAK
McCLELLAND
MAIER
&
NEUSTADT
P.C.

ATTORNEYS AT LAW

GREGORY J. MAIER
(703) 413-3000
GMAIER@OBLON.COM

RAYMOND F. CARDILLO, JR.
(703) 413-3000
RCARDILLO@OBLON.COM

October 17, 2002

SENT BY FAX

NO OF PAGES: 14
FAX #: (703) ~~305-0595~~ 308-7722

PLEASE DELIVER TO: Examiner Anh D. Mai

GROUP ART UNIT: 2814

From: Raymond F. Cardillo, Jr.

Re: Application Serial No. 09/358,388

Enclosed please find comments on 35 U.S.C. §112, first paragraph rejection and suggested amendments to overcome the rejection of Claims 44 and 45 under the second paragraph of 35 U.S.C. §112 to be discussed at the interview tomorrow at 11:00 A.M.

If you have any questions, please feel free to contact me at my telephone no. (703) 412-6508.

FAX COPY RECEIVED
OCT 17 2002
TECHNOLOGY CENTER 2800

Namely, the respective Raman intensities measured in the wave number region ranging from 300 cm^{-1} to 700 cm^{-1} as shown in Figs. 6A and 6B of the original disclosure are clearly repr senting the feature of the Raman spectra of a non doped silicon oxide film deposited by CVD

using the non doped organic silicon source. Because if the measured silicon oxide film had contained boron, the Raman spectra should have a peak at 670 cm^{-1} (See Fig.3 and table 3 of attached reference). And if the measured silicon oxide film had contained phosphorus, the Raman spectra should have a peak at 520 cm^{-1} (See Fig.4 and table 4 of the same attached reference). As we can see no peak at 670 cm^{-1} or 520 cm^{-1}, we can conclude that the Raman spectra shown in Figs. 6A and 6B of the original disclosure correspond to the data obtained from pure silicon oxide film.

Page 3, lines 32-36 of the original Specification state ".....", it is difficult in the existing state to obtain high purity organic silicon source because of limitation in a material refining technique for the organic silicon source", indicating that present invention pertains to the high purity organic silicon source. As experts in the semiconductor technology can easily understand, the term "non doped" means that the material does not contain shallow acceptor such as boron nor shallow donor such as phosphorus, which are electrically active in the semiconductor materials. It is common that if TEOS contains boron and phosphorus, it is called with acronym such as "BPTEOS" or "doped TEOS", clearly distinguishing from "TEOS"(See column 4, lines 31-38 in *Lee et al.*). That is, the experts clearly understand that the term "TEOS" means non-doped TEOS.

Although page 19, lines 30-36 state ".... oxidizing agent such as N_2O, O_2, or O_3 is added may also be employed. In addition, the grooves 6 may be buried by the silicon oxide film in terms of CVD using, as source material, organic silicon source, silicon-hydrogen compound such as SiH_4, or silicon chloride such as $SiCl_4$ alone" and page 28, lines 11-18 state "the organic silicon source into which oxidizing agent, for instance, N_2O, O_2, or O_3 is added may also be used. In addition, in terms of CVD using organic silicon source, silicon hydrogen compound such as SiH_4, or silicon chloride such as $SiCl_4$.....", there is no disclosure that the boron and phosphorus are contained.

Therefore the Examiner's contention that the original disclosure does not support the claim limitation of "a non doped organic silicon source" is clearly incorrect.

W cannot accept the Examiner's assertion that the claim limitations of "***not to include any nitride film***" and "depositing oxide film directly on the thin thermal oxidation films" are not supported by original disclosure.

Page 19, lines 22-26 state as follows:

"Then, as shown in FIG. 3B, an oxide film 7 is deposited using organic silicon source such as TEOS ($Si(OC_2H_5)_4$) after the substrate is rinsed. Prior to deposition of the oxide film 7, a thin thermal oxidation film or Si_3N_4 film may be grown."

Although the term "directly" is not found in the original disclosure, it is evident that an oxide film 7 is directly deposited on the substrate 5 as shown in Fig. 3B. In Fig.3B, there is no extra film between the oxide film 7 and the substrate 5. Since the original disclosure does not state that "a thin thermal oxidation film or Si_3N_4 film must be grown", we can optionally elect the embodiment in which the oxide film 7 is directly deposited on the substrate 5, instead of another embodiment in which the oxide film 7 is deposited on the substrate 5 through the or Si_3N_4 film.

Although the Examiner contends that the original specification does not support the term "narrower than 0.5 μm", this contention is incorrect since the grooves having the width narrower than 0.5 μm are disclosed on page 19, lines 10-14, on page 27, line 34 to page 28, line 4, which show the width of 0.3 μm. Figs. 5 and 9 disclose L/S=0.35 μm/0.35 μm, which means the width of the groove is 0.35 μm.

Page 6, line 6 to page 7, line 8, page 29, lines 25-35, and Fig. 11 show that defect density is reduced at an aspect ratio of less than 10. As page 19, line 10-14 state depth of 1 μm, the grooves can have a width of 0.1 μm to keep the aspect ratio of less than 10.

Furthermore, Eq. (3) shown on page 7 prescribe the relation:

$$l_1/l_2 \leq 1.5 \qquad \ldots\ldots (3)$$

where l_1 is the width of groove and l_2 is the width of the device region (SDG r gion) sandwiched by the grooves. Since, for example, page 11, lines 10-16 state the width of the device region is 0.3 μm, the width of groove must be less than or equal to 0.2 μm to satisfy the Eq. (3).

Therefore, it is evident that the original specification does support the term "narrower than 0.5 μm".

As to the Claim Objection that the terms "insulating material" should be changed to - - insulating film - -, we accept the amendment suggested by the Examiner in Claims 44 and 45.

Journal of Non-Crystalline Solids 45 (1981) 115–126
North-Holland Publishing Company

RAMAN SPECTRA OF BINARY HIGH-SILICA GLASSES AND FIBERS CONTAINING GeO_2, P_2O_5 AND B_2O_3

Noriyoshi SHIBATA, Masaharu HORIGUDHI and Takao EDAHIRO

Ibaraki Electrical Communication Laboratory, Nippon Telegraph and Telephone Public Corporation, Tokai, Ibaraki-ken, 319-11 Japan

Received 18 August 1980
Revised manuscript received 20 January 1981

The Raman spectra of binary high-silica glasses have been studied. The main peaks at 808 cm^{-1} and 710 cm^{-1} in vitreous B_2O_3 and vitreous P_2O_5, respectively, are greatly reduced in binary high-silica glass, whereas a peak at 425 cm^{-1} due to Ge–O–Ge vibration and a peak at 1320 cm^{-1} due to P = O vibration remain strong, increasing in intensity with decreasing SiO_2 concentration. In the stimulated Raman spectra of a P_2O_5–SiO_2 glass fiber pumped by a mode-locked and Q-switched Nd:YAG laser at 1.064 μm, strong Stokes emissions due to the P = O vibration have been observed at 1.24 μm and 1.48 μm. In the spectra for a GeO_2–SiO_2 glass fiber, four narrow-width Stokes emissions due to the Ge–O–Ge vibration have been observed at 1.115, 1.172, 1.235 and 1.305 μm.

1. Introduction

High-silica glasses containing GeO_2, B_2O_3 and P_2O_5 are well recognized as the most promising fiber materials for optical communication systems because of their low optical attenuation [1]. Infrared absorption spectra of doped fused silica were recently studied to find the attenuation limit in optical fiber [2,3] and to investigate the glass structures of binary films [4–6]. Few Raman spectroscopic studies have been made on doped fused silica, however, except for investigations concerning bond defects in the glasses [7,8]. Raman spectroscopic study will give additional structural data on doped silica glasses, because the Raman spectra of the dopants are less masked and overshadowed in the vicinity of 1100 cm^{-1} [7] than the infrared absorption spectra [6].

Stimulated Raman scattering in silica fibers have recently aroused a great interest, because the light is continuously tunable over a wide wavelength range [9–12]. It is known that the relative Raman scattering cross sections of vitreous GeO_2, B_2O_3 and P_2O_5 (abridged to v-GeO_2, v-B_2O_3 and v-P_2O_5, respectively) are 5–10 times stronger than that of vitreous SiO_2 (abridged to v-SiO_2) [13]. The superior scattering strength f the three glasses suggests that they can be used in silica fibers as the materials for increasing the gain and tuning range of fiber Raman lasers [14].

0022-3093/81/0000–0000/$02.50

We rep rt the results f a study f the spontaneous Raman scattering spectra of binary GeO_2–SiO_2, B_2O_3–SiO_2 and P_2O_5–SiO_2 glass systems over the composition range 70–100 mol.% SiO_2. Stimulated Raman spectra of binary high-silica glass fibers have also been studied. Structural information on the glasses has been obtained from their Raman spectra. The effects of the incorporation of GeO_2, B_2O_3 and P_2O_5 into SiO_2 on the Raman scattering cross sections of glass and fibers have also been clarified.

2. Experimental

2.1. Samples

Binary high-silica glasses were prepared by the VAD techniques [15]. The $SiCl_4$ vapor mixed with $GeCl_4$, $POCl_3$, and BBr_3 vapor was introduced into an oxyhydrogen flame. Synthesized porous glass rods were consolidated to bubble -free transparent glass rods in an electric furnace. As-grown glass rods were typically of 2 cm in diameter and 10 cm long. The glass composition was determined by wet chemical analysis. The OH content of the synthesized glass was about 30 ppm. Glass specimens were cut from the rods, and all their hexagonal faces were polished. Non-doped fused silica specimens were prepared from rods of Suprasil W2, Heralux and VAD-synthesized glass. Glasses containing more than 20 mol.% P_2O_5 were also prepared by conventional crucible methods.

2.2. Measurement of Raman spectra

Spontaneous Raman spectra were measured with a Coherent Radiation model-53 argon ion laser using approximately 2 W 5145 Å radiation. Scattered light at right angles from a specimen was observed through a JASCO R-500 double monochromator. The samples were positioned in the excitation beam with polished faces perpendicular to the optical plane formed by the excitation direction, and the direction in which the scattered radiation was collected. The light signal detected by an HTV R-649 photomultiplier, which was cooled at −15°C, was processed by a data-processor and was amplified. The spectra were plotted on a recorder chart. All measurements were carried out at room temperature.

Stimulated Raman emissions were measured by exciting binary high-silica fibers with a Nd:YAG laser with a peak power of 500 W. The Nd:YAG laser emitting 1.064 μm radiation is acousto-optically mode-locked at 300 MHz and is simultaneously Q-switched at 1 kHz. The pumping light pulses were focused by a 20× microscope bjective lens into a low-loss multimode fiber. The fabrication of the fibers has been reported in previous studies [15,16]. The GeO_2–SiO_2 glass core fiber is 358 m long, and the refractive-index difference, Δ, between an 84 μm-diameter core and pure silica cladding is 2.7%. The

P_2O_5–SiO_2 glass core fiber is 794 m long, and the difference, Δ, between a 60 μm-diameter core and B_2O_3-doped silica cladding is 1.2%. The output from the fibers was sent through a near-infrared grating monochromator and was detected with a Ge:APD. Detected singles were viewable on a real-time oscilliscope.

3. Results and discussions

3.1. Spontaneous Raman spectra

3.1.1. Pure fused silica (S-glass)

The Raman spectrum of S-glass is shown in fig. 1. The spectrum was used as a reference for the binary high-silica glasses. The spectra from Suprasil W2 (1 ppm OH content), Heralux (170 ppm OH content) and VAD-synthesized silica (30 ppm OH content) were quite similar in the region of 200–2000 cm^{-1}. Tetrahedral SiO_4 units, which constitute S-glass, have four normal vibrational modes [18]. The spectral components in fig. 1 correspond to those published in the literature [18–21]. The bands at 440 cm^{-1} and 485 cm^{-1} are associated with the transverse optical (TO) mode and the longitudinal optical (LO) mode of Si–O–Si bond bending vibrations (ν_4), respectively [20]. The band at 800 cm^{-1} is associated with O – Si – O symmetric bond stretching vibration (ν_1). The bands at 1060 cm^{-1}, and 1200 cm^{-1}, are respectively associated with the TO mode, and LO mode, of the O–Si–O asymmetric bond stretching vibration (ν_3). According to Bates et al. [21], the Raman band observed at 604 cm^{-1} is due to the electronic defect structure represented as $Si^+ \ldots O^- —Si$. The weak bands at 900 cm^{-1} and 1600 cm^{-1} can be attributed to the overtones and combination bands of the fundamental vibration (see table 1).

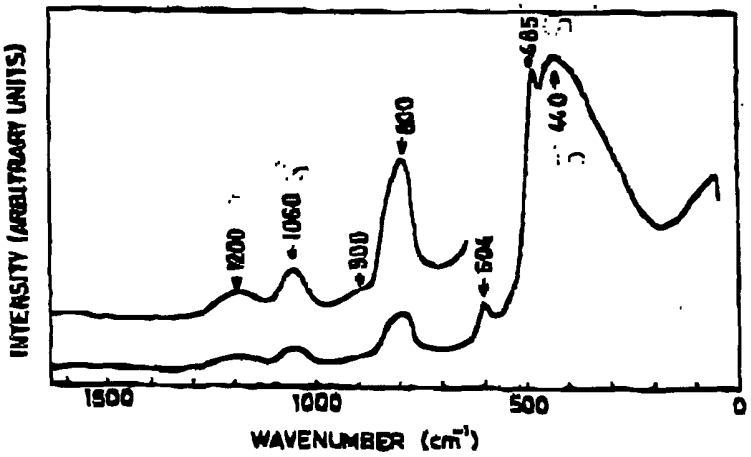

Fig. 1. Raman spectrum of pure fused silica.

Table 1
Raman and infrared peak in pure fused silica (s = strong, m = medium, w = weak and v = very)

Raman (cm^{-1})	Infrared [18] (cm^{-1})	Assignment [18–21]
440 vs	440 s	ν_4(TO): Si–O–Si bond-bending vibration
485 vs		ν_4(LO): Si–O–Si bond-bending vibration
605 m		$Si^+ \ldots O^- — Si$
800 s	810 m	ν_1: Si–O–Si bond-stretching vibration
900 vw		($2\nu_4$)
1060 w	1060 vs	ν_3(TO):Si–O–Si bond-stretching vibration
1200 w	1180 m	ν_3(LO): Si–O–Si bond-stretching vibration
1600 vw		($2\nu_1$, $\nu_3 + \nu_4$)

3.1.2. Binary GeO_2–SiO_2 glass (G-glass)

The Raman spectrum of G-glass containing 19 mol.% GeO_2 is shown in fig. 2. Raman bands which are not found in S-glass arise at 425, 580, 675, 880, 1000 and 1100 cm^{-1}. Two of the bands at 675 and 1000 cm^{-1} have been reported by Walrafen et al. [7].

Some of these bands can be assigned to the bands found in the Raman and IR spectra of pure v-GeO_2 [4,13,20] (see table 2). It is reported that pure v-GeO_2 comprises a random network of tetrahedral GeO_4 units. they have four normal vibration modes like the tetrahedral SiO_4 units. Incorporation of GeO_2 into fused silica increases the Raman scattering cross section remarkably near 430 cm^{-1}, as can be seen in fig. 2. A strong band at 425 cm^{-1}, which is IR inactivity [19], may be associated with bond-rocking motion: oxygen atoms move perpendicular to the Ge–O–Ge plains [22]. The band at 580 cm^{-1}, which may correspond to an IR peak at 550 cm^{-1}, is associated with the Ge–O–Ge symmetric bond stretching vibration (ν_1). The band at 800 cm^{-1} is associated with the Ge–O–Ge asymmetric bond stretching vibration (ν_3).

The Raman bands at 675 cm^{-1} and at 1000 cm^{-1}, which were absent both in the spectra of S-glass and pure v-GeO_2, may be associated with the stretching vibration of the Ge–O–Si chain. This indicates that there is an interconnected structure of GeO_4–SiO_4 tetrahedra [4]. A new band found at 1100 cm^{-1} increases in intensity with increasing GeO_2 content.

3.1.3. Binary B_2O_3–SiO_2 glass (B-glass)

The Raman spectrum observed for B-glass containing 10 mol.% B_2O_3 is shown in fig. 3. Raman bands due to the introduction of B_2O_3 appear at 450, 670, 720, 800, 925, 1130 and 1360 cm^{-1}. Two of the bands at 940 cm^{-1} and 1130 cm^{-1} have been reported by Walrafen et al. [7].

Some of the bands in fig. 3 correspond to the spectral components in the reported Raman [13,23] and IR [5] studies on pure v-B_2O_3 (see table 3). According to the literature, pure v-B_2O_3 is thought to be a random netw rk of planar BO_3 units. The normal vibration frequencies of BO_3 units strongly resemble that of planar BF_3 molecules [24]. The strong band at 450 cm^{-1},

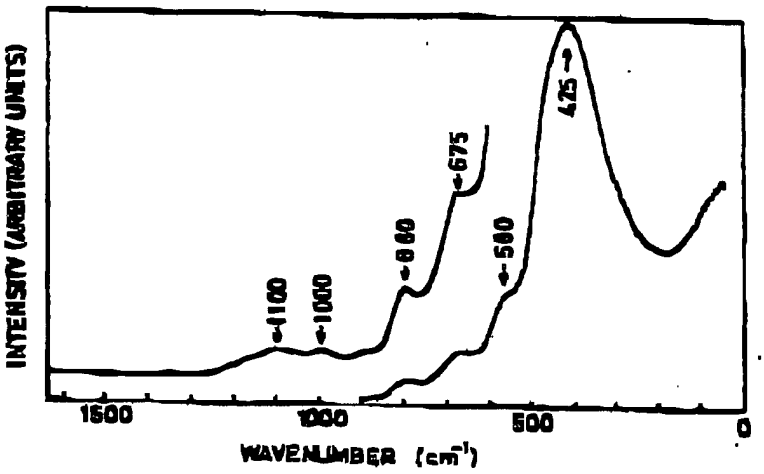

Fig. 2. Raman spectrum of binary GeO_2–SiO_2 glass containing 19 mol.% GeO_2.

which could not be seen in IR spectra of binary B_2O_3–SiO_2 glasses [5], is associated with the B–O–B bond bending vibration (ν_4): the atoms move in the BO_3 plane. The very weak band at 720 cm^{-1}, which can be observed in the glass containing B_2O_3 as high as 20 mol.%, is associated with the B–O–B bond bending vibration (ν_2): the atoms move perpendicularly to the BO_3 plane. The B–O–B symmetric bond stretching vibration (ν_1), which brings about the strongest line at 800 cm^{-1} in the Raman spectra of pure v-B_2O_3 [23], corresponds to no strong line in the Raman spectra of B-glass. The reduction of the symmetric component in the B–O–B bond stretching vibration may be attributed to the incorporation of B_2O_3 into SiO_2. The broad band at 1360 cm^{-1} is associated with the B–O–B asymmetric bond stretching vibration (ν_3) [23]. The Raman bands at 670 cm^{-1} and 925 cm^{-1}, which are absent in the spectra of fused silica and pure v-B_2O_3, are respectively associated with the B–O–Si bond bending and bond stretching vibration [5].

The marked differences in the Raman spectra between v-B_2O_3 and B-glass,

Table 2
Observed Raman frequency in GeO_2-doped fused silica (s = strong, m = medium, w = weak, v = very)

Raman (cm^{-1})	Infrared [4] (cm^{-1})	Assignment
425 vs		Ge–O–Ge bond-rocking motion
580 m	550 m	ν_4: Ge–O–Ge bond-stretching vibration
675 s	675 w	Ge–O–Si bond-stretching vibration
880 vw	870 s	ν_3: Ge–O–Ge bond-stretching vibration
1000 w	1000 s	Ge–O–Si bond-stretching vibration
1100 m		

6/13

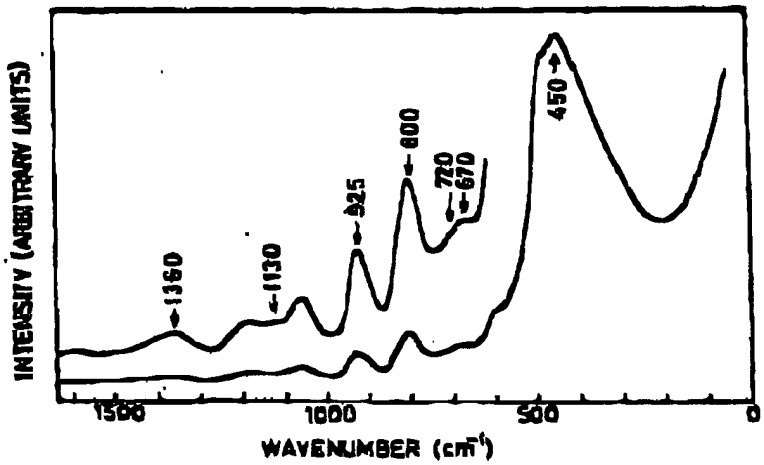

Fig. 3. Raman spectrum of binary B_2O_3–SiO_2 glass containing 10 mol.% B_2O_3.

namely the ν_3 band shift and ν_1 band intensity change, can be ascribed to the fact that planar BO_3 units in B-glass form a continuous network together with tetrahedral SiO_4 units, and slightly deform to reduce C_{3v} symmetry.

3.1.4. *Binary P_2O_5–SiO_2 glass (P-glass)*

The Raman spectra observed for P-glass containing 14 mol.% and 30 mol.% P_2O_5 are given as curves (a) and (b), respectively, in fig. 4. Raman bands due to the introduction of P_2O_5 appear at 300, 420, 520, 710, 800, 1020, 1145, 1200 and 1320 cm^{-1}. The measured frequency and intensity of the bands due to P_2O_5 molecules differ greatly from those in the Raman spectra of pure v-P_2O_5 reported by Galeener et al. [25], but show some resemblance to those reported by Bobovich [26]. Galeener's sample of v-P_2O_5, which was prepared by condensing vapor, showed some aspects of the rhombohedral P_4O_{10} molecular structure. Since the band maximum frequencies of P-glass shown here have some resemblance to the IR absorption peaks of CVD-deposited binary

Table 3
Observed Raman frequency in B_2O_3-doped fused silica (s = strong, m = medium, w = weak, v = very)

Raman (cm^{-1})	Infrared [5] (cm^{-1})	Assignment
450 s		ν_4: B–O–B bond-bending vibration
670 w	670 m	B–O–Si bond-bending vibration
720 vw	720 w	ν_4: B–O–B bond-bending vibration
800 vw		ν_1: B–O–B bond-stretching vibration
925 m	930 m	B–O–Si bond-stretching vibration
1130 vw	1130 s	
1360 w	1360 vs	ν_3: B–O–B bond-stretching vibration

7/13

P_2O_5–SiO_2 glass films [6], the phosphorus atoms may have a configuration of PO_4 tetrahedra. In the tetrahedral PO_4 units nly three of the oxygen atoms f each unit bridge to neighboring units, while the fourth is double-bonded to the central phosphorus atom.

The observed band could be assigned to vibration modes in the glass. The assignments listed in table 4 were suggested by comparing our data with the IR spectra of P-glass [6] and vibration modes of quasi-tetrahedral XY_3Z-type molecules having one double-bonded oxygen atom, such as POF_3 molecules [23]. Based on the IR study [6], the 1320 cm^{-1} peak in fig. 4 is assigned to the P=O bond. The Raman bands at 1200 cm^{-1} and 800 cm^{-1} may be associated with the stretching vibration of P–O–P units. The 800 cm^{-1} peak due to the P–O–P vibration is very weak in the Raman spectra of P-glass. The Raman bands at 710 cm^{-1} and 520 cm^{-1} may be associated with bending vibration of O=P–O and O–P–O units, respectively. Incorporation of P_2O_5 into SiO_2 greatly reduced the Raman peak corresponding to the 640 cm^{-1} peak in v-P_2O_5. In P-glass containing smaller amount of P_2O_5, the Raman peak at 440 cm^{-1} seen in fig. 1 shifts to 420 cm^{-1} and boadens. A shoulder band appears near 300 cm^{-1} [this can be seen in curve (a) in fig. 4]. A band was also observed at 1145 cm^{-1}. It may be associated with Si–O–P bond stretching vibration.

All the Raman spectra of P-glass indicate that P-glass is made up of a random network of tetrahedral SiO_4 units and tetrahedral PO_4 units.

3.1.5. Variation of scattering intensities with composition

Raman scattering cross sections of v-SiO_2, v-GeO_2, v-B_2O_3 and v-P_2O_5 have relative strengths of 1.0 (at 444 cm^{-1}), 9.2 (at 420 cm^{-1}), 4.7 (at 808 cm^{-1}), and 5.7 and 3.5 (at 640 cm^{-1} and 1390 cm^{-1}), respectively [13]. It is interesting

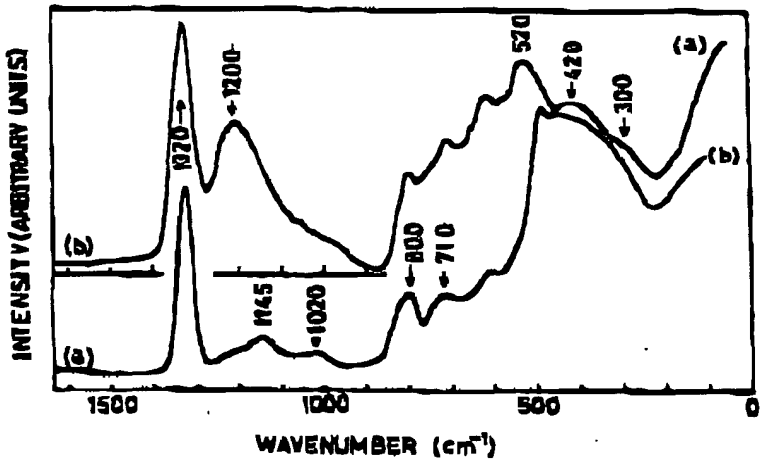

Fig. 4. Raman spectrum of binary P_2O_5–SiO_2 glasses containing (a) 14 mol.% P_2O_5 and (b) 30 mol.% P_2O_5.

8/13

Table 4
Observed Raman frequency in P_2O_5-doped fused silica (s = strong, m = medium, w = weak, v = very)

Raman (cm^{-1})	Infrared [6] (cm^{-1})	Assignment
300 w		
420 s		
520 m	475 s	ν_6: O–P–O bond-bending vibration
710 m	650 w	ν_4: O = P – O bond-bending vibration
800 vw	780 vw	ν_3: P–O–P bond-stretching vibration
1020 w	950 s	ν_2: P–O–P bond-stretching vibration
1145 m	1100 s	P–O–Si bond-stretching vibration
1200 m	1150 s	ν_5: P–O–P bond-stretching vibration
1320 vs	1320 m	ν_1: P = O bond-stretching vibration

to examine whether these peaks also have strong cross sections in binary glass systems. The 800 cm^{-1} peak of Si–O–Si bond stretching vibration was used as a standard for the relative Raman cross section of the binary high-silica glasses.

The 430 cm^{-1} peak has the strongest cross section in G-glass. This peak may be caused by a superposition of the 440 cm^{-1} peak of SiO_2 and the 425 cm^{-1} peak of GeO_2. The assumption that the two peaks contribute independently to the increase of the 430 cm^{-1} peak intensity in proportion to mole concentration explains the G-glass cross section shown in fig. 5 well. In B-glass, however, incorporation of B_2O_3 into SiO_2 greatly reduces the 808 cm^{-1} peak. No stronger peak due to B_2O_3 molecular vibration was observed. Incorporation of P_2O_5 into SiO_2 greatly reduces the Raman peak corresponding to the 640 cm^{-1} peak in v-P_2O_5. The P = O band seen at 1320 cm^{-1} increases, on the other hand, in intensity proportional to P_2O_5 concentration (this is shown in fig. 6). Extrapolation to 100% P_2O_5 produces the result that agrees well with the relative intensity of 1390 cm^{-1} peak reported by Galeener et al.

With respect to the Raman lines of Ge–O–Si, B–O–Si and P–O–Si linkages in the binary glasses, all bands increase in intensity over the observed composition range with decreasing SiO_2 concentration. The relative Raman intensities for the main bands of each linkage are shown in fig. 7 as a function of composition. The Raman intensity of the linkages is, however, much smaller than the 440 cm^{-1} peak in v-SiO_2.

3.2. Stimulated Raman scattering

The large Raman cross sections for P-glass and G-glass suggest that the glasses should have a lower threshold level f stimulated Raman scattering, and exhibit str ng higher- rder Stokes emissi ns.

A stimulated Raman scattering spectrum obtained fr m a multimode with a P_2O_5–SiO_2 glass c re containing 25 mol.% P_2O_5 is shown in fig. 8. This

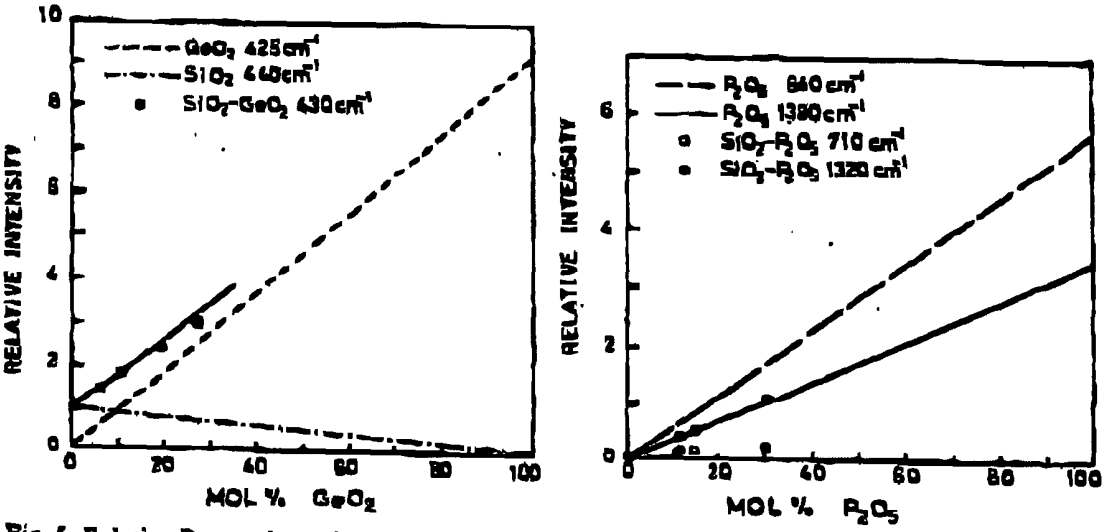

Fig. 5. Relative Raman intensity at the band maximum of the 430 cm^{-1} band in G-glass (●) as a function of composition. Peak intensities of the 425 cm^{-1} and 440 cm^{-1} bands are simply extrapolated from the values of vitreous-GeO_2 and vitreous-SiO_2, respectively, as measured by Galeener et al. [13].

Fig. 6. Relative Raman intensities at the band maximum of the 710 cm^{-1} and 1320 cm^{-1} bands in P-glass as a function of composition. Peak intensities of the 640 cm^{-1} and 1390 cm^{-1} bands are simply extrapolated from the values of vitreous-P_2O_5 measured by Galeener et al. [13].

particular P_2O_5–SiO_2 glass fiber has a loss of 1.8 dB/km at the 1.064 μm pump-laser wavelength and a loss well below 5 dB/km at 0.8 to1.6 μm. In fig. 8, the spectrum of the generated continuum shows the pump, the first and second Stokes shifts due to the P=O mode near 1.24 μm and 1.48 μm, the

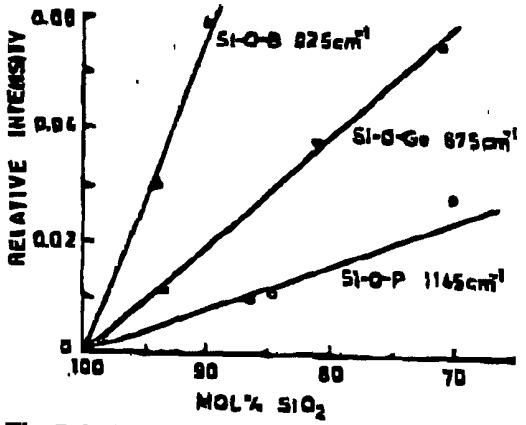

Fig. 7. Relative Raman intensities of Ge–O–Si, B–O–Si and P–O–Si linkages in binary glasses as a function of composition.

10/13

first Stokes shift due to the Si–O–Si mode near 1.12 μm (460 cm^{-1}), and the combinations of the two modes near 1.3 μm. The St kes shifts corresponds t the P = O stretching mode at 1320 cm^{-1}. The spectrum in fig. 8 shows more clearly the influence of P_2O_5 than the result previously reported by Grigoryyants et al. [14]. The present results confirm that the addition of a fair amount of P_2O_5 to fused silica can greatly lower the threshold level of stimulated Raman scattering and generate strong Stokes emissions in the region above 1300 cm^{-1}. The spectra obtained from a multimode fiber with a GeO_2–SiO_2 core containing 27 mol.% GeO_2 is shown in fig. 9. This fiber has a loss of 1.7 dB/km at 1.064 μm and a loss well below 2 dB/km at 1.0 to 1.7 μm, except for the loss peak due to OH absorption in the vicinity of 1.4 μm. In fig. 9 the spectra of the generated continuum show the pump, the first four narrow-width Stokes shifts at 1.115, 1.172, 1.235 and 1.305 μm, and the higher order Stokes shift out to 1.8 μm. The Stokes shifts, which are in the region of 430–436 cm^{-1}, suggest that these lines correspond to the vibration mode of GeO_4 tetrahedra. This result also confirms that addition of GeO_2 to fused silica can greatly lower the threshold level of stimulated scattering

It has been known for some time that a low threshold level for stimulated Raman scattering in optical fibers can be achieved with: (a) a small core cross section; (b) low transmission loss; and (c) high non-linear effect gain coefficient [27]. Application to a fiber Raman laser requires further; (d) a sharp emission pulse with a small distortion. A silica-based single-mode fiber is a preferred candidate in order to fulfill the above conditions [9–12]. It is

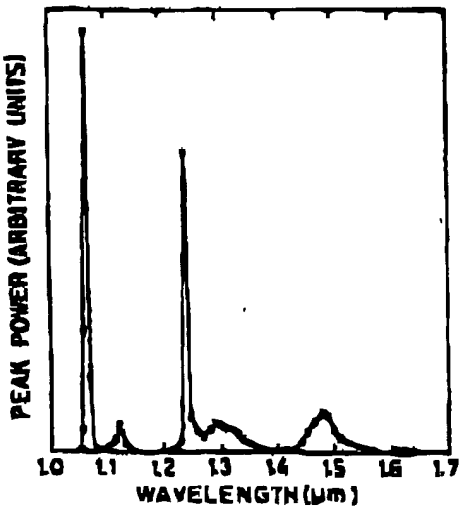

Fig. 8. Stimulated Raman scattering spectrum obtained from a multimode fiber with a P_2O_5–SiO_2 glass core containing 25 mol.% P_2O_5.

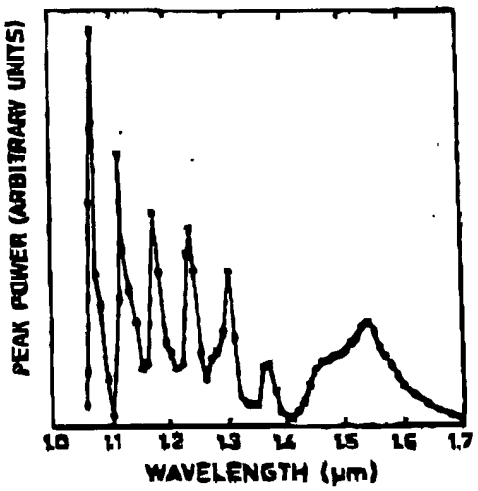

Fig. 9. Stimulated Raman scattering spectrum obtained from a multimode fiber with a GeO_2–SiO_2 glass core containing 27 mol.% GeO_2.

11/13

strongly expected that single-mode fibers with a high-silica core containing a large amount of P_2O_5 and GeO_2 are good candidates for fiber Raman lasers having a high gain over a wide spectral range. Other candidates could be a pure-GeO_2 core single-mode fiber, or a high GeO_2- and P_2O_5-content silica core multimode fiber with broad transmission bandwidth over the 1.0 to 2.0 μm region.

4. Conclusions

The Raman spectra of binary GeO_2-SiO_2, $B_2O_3-SiO_2$ and $P_2O_5-SiO_2$ glass systems have been systematically studied with reference to pure fused silica spectra. It is confirmed that the molecules in the glass network have such configurations as tetrahedral SiO_4 units, tetrahedral GeO_4 units, planar BO_3 units, and tetrahedral PO_4 units in which one of the oxygen atoms is doubly bonded to the phosphorus atom. The addition of other components to fused silica is found to have remarkable effects on the Raman spectra, especially in P-glass and B-glass. Raman bands indicative of the bonding of SiO_2 and additional materials were observed: Ge–O–Si modes at 675 cm^{-1} and 1000 cm^{-1}, B–O–Si modes at 670 cm^{-1} and 1000 cm^{-1}, and a P–O–Si mode at 1145 cm^{-1}. The main peaks at 808 cm^{-1} and 710 cm^{-1} in v-B_2O_3 and v-P_2O_5, respectively, were greatly reduced in binary high-silica glasses, whereas a peak at 425 cm^{-1} due to a Ge–O–Ge vibration and a peak at 1320 cm^{-1} due to a P=O vibration remain strong, increasing in intensity with decreasing SiO_2 concentration.

Stimulated Raman spectra have also been obtained from some of the samples in fiber form. The results proved that introduction of GeO_2 and P_2O_5 into fused silica can increase fiber Raman laser gain. A low-loss single-mode fiber with high-silica core containing a large amount of GeO_2 and P_2O_5 is applicable to a fiber Raman laser for a high gain and wide tuning ranges.

The authors would like to express their appreciation to N. Niizeki, H. Takata and N. Inagaki for continuous encouragement. They also thank S. Takahashi and M. Kawachi for valuable discussions, and Y. Ohmori for supplying the binary $P_2O_5-SiO_2$ glass fiber.

References

[1] T. Miya, Y. Terunuma, T. Hosaka and T. Miyashita, Electron. Lett. 14 (1978) 534.
[2] T. Izawa, N. Shibata and A. Takeda, Appl. Phys. Lett. 31 (1977) 33.
[3] H. Osanai, T. Shioda, T. Moriyama, S. Araki, M. Horiguchi, T. Izawa and H. Takata, Electron. Lett. 12 (1976) 549.
[4] N.F. Borrelli, Phys. and Chem. Glasses 10 (1969) 43.
[5] A.S. Tenney and J. Wong, J. Chem. Phys. 56 (1972) 5516.
[6] J. Wong, J. Non-Crystalline Solids 20 (1976) 83.

[7] G.E. Walrafen and J. Stone, Appl. Spectr. 29 (1975) 337.
[8] D. Kato, J. Appl. Phys. 47 (1976) 2050.
[9] R.H. Stolen, E.P. Ippen and A.R. Tynes, Appl. Phys. Lett. 20 (1972) 62.
[10] K.O. Hill, B.S. Kawasaki and D.C. Johnson, Appl. Phys. Lett. 29 (1976) 181.
[11] G. Cohen and Chinlon Lin, Appl. Opt. 16 (1977) 3316.
[12] Chinlon Lin, V.T. Nguyen and W.G. French, Electron. Lett. 14 (1978) 822.
[13] F.L. Galeener, J.C. Mikkelson, Jr., R.H. Geils and W.J. Mosby, Appl. Phys. Lett. 32 (1978) 34.
[14] V.V. Grigoryyants, B.L. Davydov, M.E. Zhabotinski and V. Chamorovski, Opt. Quant. Elect. 9 (1977) 351.
[15] T. Izawa, S. Sudo and F. Hanawa, Trans. IECE Jpn. E62 (1979) 779.
[16] N. Shibata, M. Kawachi, S. Sudo and T. Edahiro, Electron. Lett. 15 (1979) 680.
[17] Y. Ohmori, H. Okazaki, I. Hatakeyama and H. Takata, Electron. Lett. 15 (1979) 616.
[18] W. Wadia and L.S. Ballomal, Phys. Chem. Glasses 9 (1968) 115.
[19] I. Simon, in: Modern aspects of the vitreous state, Vol. 1, ed., J.D. Mackenzie (Butterworths, London, 1960) p. 120.
[20] F.L. Galleher and G. Lucovsky, Phys. Rev. Lett. 37 (1976) 1474.
[21] J.B. Bated, R.W. Hendrick and L.B. Shaffer, J. Chem. Phys. 61 (1974) 1474.
[22] M. Hass, J. Phys. Chem. Solids 31 (1970) 415.
[23] J.P. Bronswijk and E. Sirijks, J. Non-Crystalline Solids 24 (1977) 145.
[24] K. Nakamoto, Infrared spectra of inorganic and coordination compounds (Wiley, New York, 1973) p. 97.
[25] F.L. Galleher and J.C. Mikkelsen, Jr., Sol. St. Comm. 30 (1979) 505.
[26] Y.S. Bobovich, Opt. Spectry. (Engl. Transl.) 13 (1962) 274.
[27] R.G. Smith, Appl. Opt. 11 (1972) 2489.